METHODS OF EARTHQUAKE-PROOF SAFETY DESIGN FOR PLANT STRUCTURE AND COST REDUCTION OF A PIPE RACK IN LNG PLANTS

Takenori Makita, Managing Director,
Tatsuya Hasegawa, Manager, Hajime Anzai, Deputy Manager
Nihonkai LNG Co. Ltd.
1612-32, Higashiko Seiromachi 1 Chome Kita-Kanbaragun, Niigata 957-0195 Japan

KeijiroYoshida, PM
Mitsubishi Heavy Industries, Ltd., Machinery Headquarters
3-1, Minatomirai 3 Chome Nishi-Ku, Yokohama 220-84 Japan

Shigemi Ochiai, Ph.D, CEO, Jonquil Consulting Inc.
1-30, Takaido-Higashi 1 Chome Suginami-Ku, Tokyo 168-0072 Japan

ABSTRACT

Since the beginning of recorded history, earthquakes have brought some truly appalling disasters upon mankind. In just the past few years we have had the Great Hanshin Earthquake in Japan, the Izmit Earthquake in Turkey, and the Cumulative Earthquake in Taiwan. These have brought untold damage to lifeline facilities needed for public services. In particular, after the Great Hanshin Earthquake it took three days for electric power to be restored and several months for the gas supply to return. This once again recognized the need for an enough investigation on the safety design of public utility facilities. Given this situation, we conducted studies and research over the space of five years from 1996 on the earthquake-proof safety design of Nihonkai LNG Niigata terminal, an important energy centre on the Japan Sea side of the country, based on the lessons from the Great Hanshin Earthquake.

The object of research was to make certain the scale of earthquakes and measures for improving the earthquake-proof safety design of various facilities. In particular, we judged that it was important to do earthquake-proof reinforcement to pipe rack in various facilities. In order to achieve this purpose, we enforced a static load and a three dimensional dynamic experiments. As a result of this research, a ductility factor of pipe rack with earthquake-proof reinforcement was about 3 times in comparison without reinforcement. In the results of research for five years, we have described the background to the pipe rack ductility factor calculated by static loading experiments. We also discuss how this ductility factor should be applied to earthquake-proof design to facilitate the assurance of earthquake-proof safety for pipe racks.

Finally, if you adopt the new model and a ductility factor of pipe rack that we suggested, you can make earthquake-proof reinforcement of existing pipe rack extremely cheap. Also if you adopt it, new pipe rack construction can reduce steel materials of 30 %.

1. Summary of studied and research works for five years

We show one part of LNG facility whole view with Photograph 1. To do this, we categorized the importance of the facilities in terms of risk management, and organized earthquake reinforcement measures in line with the level of importance. Figure 1 shows an example of screening results. As Figure 1 shows, the screening assessed 5 factors by assigning points from 1 to 5 for each factor, with 5 points representing the most dangerous state of each factor. The final risk evaluation was represented by the total of the points given to all five factors and ranking the object with the highest score as the one with the greatest influence.

Photograph.1 C14 One part of facilities in Nihonkai LNG Niigata Terminal

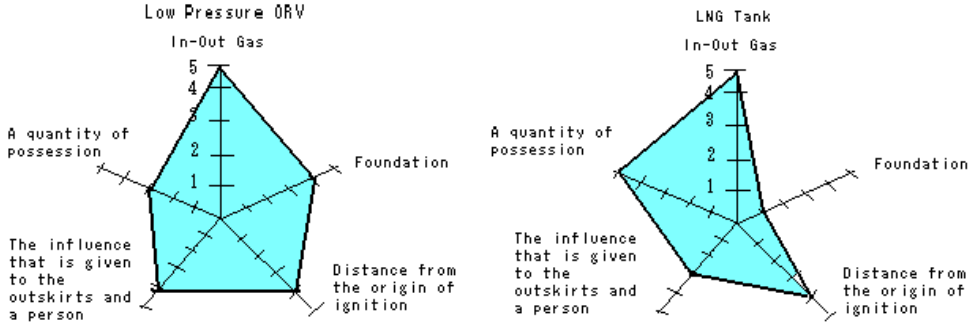

Figure 2 The result of screening

Table 1 shows facility from big order of influence degree to the fifth. This study has revealed that earthquake damage to the low pressure ORV would cause the most harm to the rest of the plant equipment. We collated the extent of damage caused by the scale of earthquakes and theories on earthquake movement, and installed strong motion seismographs in important points at each facility. We incorporated data on actual earthquake behavior recorded by the seismographs in earthquake-proof calculations. As a result, we proved that earthquake-proof safety design in pipe racks needs to be reconfirmed. We focused, in particular, on pipes from a vaporizer and the racks supporting them. We also analyzed two-dimensional liquefaction of subsoil and conducted earthquake-proof calculations taking account of the effects of liquefaction. As a result, we proved that the columns, beams, pedestals, and foundation concrete of pipe racks needs to be reinforced. In the case of columns and beams, applying a cover plate and thus increasing strength can complete reinforcement. But with the pedestals and foundation concrete, we proved that, if strengthened without due care, the pedestals will become fixed and the piles subject not only to an additional axial force but also to an excessive bending stress. Therefore, measures to reduce these are needed. To solve this, we developed a new method of reinforcing pedestals and pedestal foundations while coupling them with a cushioning material. We made a 1/3-scale model of an actual pipe rack

Table.1 Evaluation of risk

Facilities Items	Evaluation of risk
L ORV	20
L LNG Pump	19
M ORV	18
H ORV	18
LNG Tank	18

and conducted simulations on a large-scale shaking table, proving that the effects are considerable. We also conducted static loading experiments on the 1/3-scale model of an actual pipe rack and dynamic vibration experiments on a large-scale shaking table. The aim of this was to confirm the “ultimate strength of pipe racks with the developed reinforcement measures” when applying the results of these research to actual earthquake-proof reinforcement of pipe racks. As a result, we were able to quantify the ductility factor of pipe racks with earthquake-proof reinforcement. Further, in order to confirm “the effect of liquefaction on pipe racks”, we conducted large-scale shaking table experiments using the same model as above. As to the stress acting on pipe racks due to liquefaction, we found that the stress occurring at points of contact between the pipes and the pipe rack is largest at the moment when the pipes are pulled downwards simultaneously with the occurrence of liquefaction. If the ductility factor of pipe racks calculated in this research is applied to pipe racks designed for earthquake-proof reinforcement, the true yield strength of the pipe rack will be known and it will be clear how great an earthquake force factor can be covered. If the ductility factor is applied to earthquake-proof design in advance when designing new pipe racks, optimal member selection will be possible. Also, with respect to the maximum stress acting on the pipe rack due to liquefaction, it will be possible to reduce stress by placing cushioning material at points of contact between the pipes and the pipe rack. We have reflected these result and started earthquake-proof reinforcement work.

2. Briefing of the static load experiment

The earthquake-proof reinforcement sharply lowered the design allowable stress from 1.0, maintaining the safety of the pipe rack. We made a model of 1/3 size of a real pipe rack in order to know an earthquake-proof of pipe racks quantitatively. We named after Type-0 and Type-3, which are the pipe rack without reinforcement and with reinforcement. Models of pipe racks before earthquake-proof reinforcement and racks after earthquake-proof reinforcement were used for static loading experimenting in order to clarify which model exceeded the yield point and estimate their strength (ultimate strength). Photograph 2 and 3 shows these experiments.

Photograph-2 Static load experiment without reinforcement model (Type-0)

Photograph-3 Static load experiment with reinforcement model (Type-3)

Two kinds of models were anchored to a solid experiment floor and two hydraulic jacks (each 500 kN) installed on the vertical wall loaded the samples in steps through a load cell. As the hydraulic jacks loaded the models, the displacement and stress of all parts of the models were measured. The displacement was measured at the locations shown in Figure 2 by strain type displacement gauges. And the stress values of Type-0 and Type-3 were measured in the column base including the foundation concrete, the column, and the girder. Plastic gauges were used for these stress measurements, but normal strain gauges were used to measure the anchor bolts. A measurement was performed using a strain type displacement meter in order to observe the rise of the anchor plate of the type-0 frame foundation. The load and the displacement and stress referred to above were recorded in a high-speed data logger through a high-speed switch box during the experiment. During loading, the failure limits of each model were observed while the deformation and stress of every part was monitored and the loading was halted when it was assumed that failure had occurred.

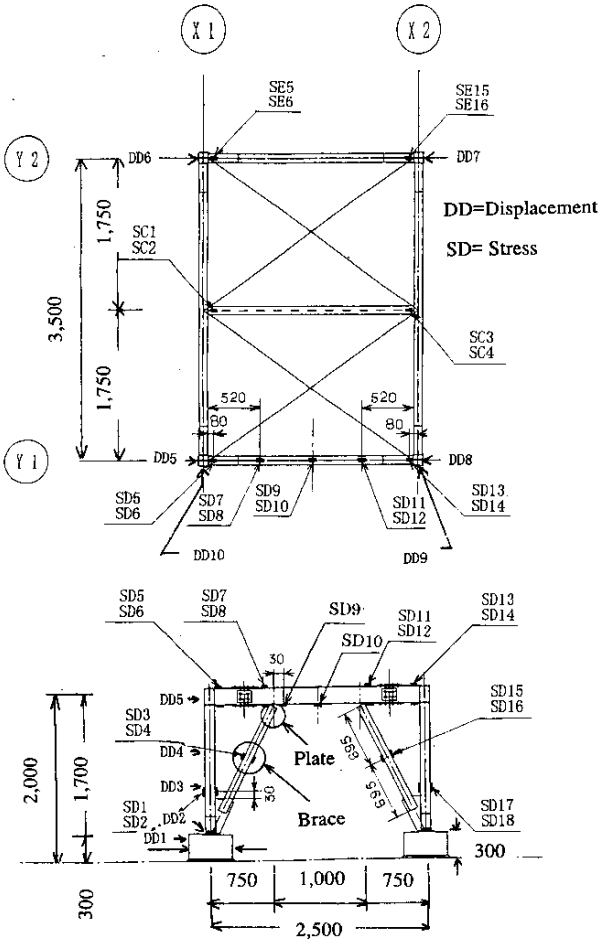

Fig,2 A measurement points of displacement by static load experiment

3. The results of ultimate strength by static loading experimenting

(1) Results of experimenting of Type-0

The model was loaded with displacement controlled by a hydraulic jack, and the state of the model was observed as the load was increased in steps of about 5 kN. Figure 3 shows the load – displacement peak during loading. No particular change of the model was observed up to approximately 25 kN, but from about 25 to 30 kN, peeling occurred between the base plate and the concrete (grout), and the subsequent rise in the load was accompanied the expansion of this gap. When the load reached 47 kN, the grout of the X1 – Y2 column foundation cracked, but no problems were observed in any other foundations. This cracking slightly lowered the load of the hydraulic jack on Y2. When the load was increased to 65 kN, the anchor bolt of the X1-Y1 column fractured with a low sound. The increase of the displacement of the hydraulic jack was continued, but because the anchor bolt of X1-Y2 column fractured without any

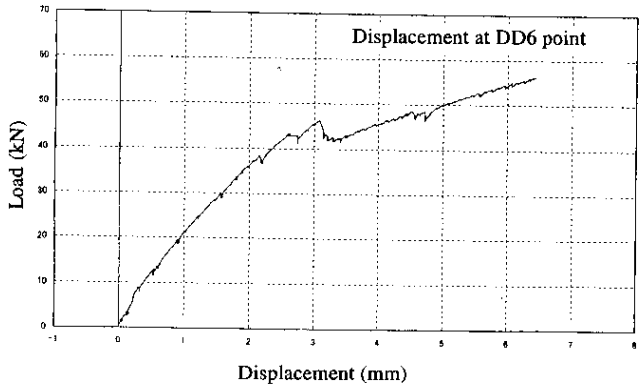

Figure 3 The curve of load-displacement at DD6 point during static load (Type-0)

Increase in the load, this time was considered to be failure and the experiment was concluded. Photograph-4 shows the state of the model during and after the experimenting.

Photograph-4 Pedestal was broken by ductile fracture (Type-0)

(2) Results of experimenting of Type-3

As the state of the model was observed, the load on the model was increased in steps under displacement control by a hydraulic jack as it was during the Type-0 experiment. Figure 4 shows the load – displacement peak during the loading. Until 64 kN, no particular change of the model was observed, but near 70 kN, a small gap was observed between the column and the filler, and as the load increased, the gap tended to widen. When the load reached 130 kN, bending could be seen at the brace on the compression side, the load peaked at 163 Kn, and then the load declined and began to rise again at 153 kN.

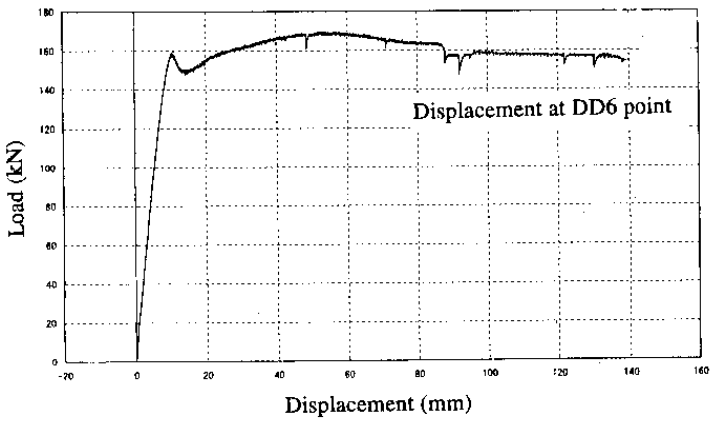

Figure 4 The curve of load-displacement at DD6 point during static load (Type-3)

4. Evaluation of results

(1) In the results of the static loading experiment of Type-0, other members were not damaged, but because the anchor bolt fractured at a load of 63 kN from figure 3, this was considered to be the failure time. The Type-3 experiment results show that at 162.6 kN the brace yielded and the load carrying capacity fell from figure 4, but although the anchor bolt, base plate, and girder yielded later, the load bearing capacity increased slightly and the anchor bolt fractured at 168.8 kN. Then the deformation of the model advanced until the column yielded, and at the same time, the load carrying capacity fell, and because the incline of the column (displacement of approximately 142 mm at the top of the column) increased at 151.9 kN, this was considered to be failure. A comparison of the maximum load carrying capacities of the two models revealed values of 63.5 kN and 168.8 kN for Type-0 and Type-3 respectively, showing that the load carrying capacity of Type-3 is about 2.6 times that of Type-0 and that the measure is remarkably effective.

(2) The fracturing of the anchor bolt on the Type-0 model during the static loading experimenting was a ductile fracture caused by the shear load. About Type-3, we made sure the inside of the model foundation after experiment. The results showed that in the foundation used for the static loading experimenting, two anchor bolts on the loading side were fractured and the center of the base plate was deformed about 7 mm upwards so it looked like a soup bowl placed face down. Photograph 5 and 6 shows an aspect after experiments.

Photograph–5 The compression braces were completely buckled by the static load experiment

Photograph-6 The beams buckled by the static load experiment (Type-3)

5. Conclusion

We have understood the following things through this research work.

(1) Maximum load carrying capacity

The maximum load capacity is recorded in the results of the experimenting. The results of a comparison of the maximum load carrying capacity of Type-0 and Type-3 are shown in table 2. As the table shows, the maximum load carrying capacities of Type-0 and Type-3 are 65.3 kN and 168.8 kN respectively, revealing that the load carrying capacity of Type-3 is about 2.6 times that of Type-0 indicating that the measure was remarkable effective. Table 2 shows a comparison of the Yield Load and Maximum Load Carrying Capacity of Type-0 and Type-3.

Table 2 Comparison of the Yield Load and Maximum

Load Carrying Capacity of Type-0 and Type-3.

Model	Yield Load (kN)	Max. Load Carrying Capacity (kN)	Displacement at the Max. Load Carrying Capacity (mm)
Type-0	25.2	65.3	6.1
Type-3	162.6	168.8	52.4

(2) Ductility factor

The ductility factor defined by the following equation has conventionally been used as one criterion to indicate earthquake-proof safety. An equation is shown (1)

$$\mu = x_u / x_y \quad (1)$$

Where:

μ: ductility factor

x_y: yield displacement

x_u: max. displacement

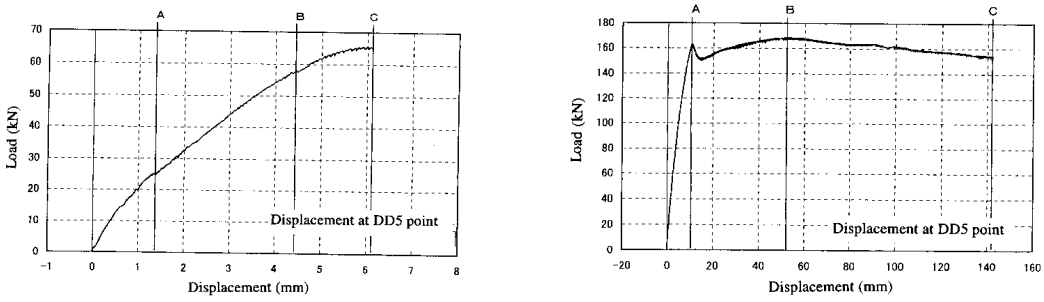

(a) (b)

Figure 5 shows the load–displacement curves of Type-0 and Type-3.

As Figure 5(a) shows, the yield point of Type-0 is unclear, but the point A of the first plastic joint that is thought to be the yield point of the anchor bolt is considered to be the yield point of Type-0. As figure 5(b) shows, the first yield point of Type-3 is A and the ultimate strength is point C. And applying the results in Figure 5 to equation (1) to find the respective ductility factors obtains the results in Table 3. As Table 3 shows, the ductility factor of Type-0 is 4.4, but that of Type-3 is larger at 13.7, revealing a ductility factor improvement of 3 times.

Table 3 Comparison of the Ductility Factors of Type-0 and Type-3

Model	Yield displacement x_y (mm)	Max. displacement x_u (mm)	Ductility factor μ
Type-0	1.38	6.12	4.4
Type-3	10.36	142.20	13.7

The execution design done to prepare for the earthquake-proof reinforcement stipulated that cover plates be installed on columns and beams with little leeway between the design allowable stress and the present design earthquake force coefficient accounting for the

ductility rate found of 3 times, that cushioning materials be inserted between the pedestal and the concrete of the pedestal foundation and that these pedestal foundations be earthquake-proof reinforcement with concrete. Earthquake-proof reinforcement of part of the pipe rack began based on this earthquake-proof reinforcement design. Photograph 7 and 8 shows the scene of the earthquake-proof reinforcement work.

Photograph -7 The earthquake-proof reinforcement work

Photograph -8 The earthquake-proof reinforcement work

The above earthquake-proof reinforcement work is going to guarantee the earthquake safety of the pipe racks at Nihonkai LNG Niigata terminal, an important energy centre on the Japan Sea side of the country. We are to complete earthquake-proof reinforcement work by 2004 years.

6. The effect of cost reduction due to the application of the earthquake-proof reinforcement method

As indicated in Section 5, it has been verified through static load experiments that it is possible to achieve three times the ductility factor of pipe racks through the application of earthquake-proof reinforcement. It has furthermore been shown to be capable of securing a seismic intensity of 0.45G or greater. In order to secure a seismic intensity of 0.45G or more in pipe racks by conventional design methods, it is necessary to increase the member size of each member to a considerable degree. This increase in the cross-sectional size would then lead to an increase in the amount of materials used as well as the construction costs. In light of the above, the benefits described below can be obtained if the earthquake-proof reinforcement method that we propose here is applied to pipe racks.

(1) In the case of existing pipe racks, if steel is applied to beams, columns and braces and rubber material is inserted in the bottom-wrapped pedestal and column base, this will result in a broad increase in the ultimate strength of the pipe rack and it will be possible to secure a seismic intensity of 0.45G or more.

(2) There is no need to reinforce the pile since new bending stress is alleviated by inserting the rubber material in the bottom-wrapped pedestal and column base.

(3) Items (1) and (2) above will also make it possible to secure a seismic intensity of 0.45G or more in existing pipe racks.

(4) Comparing the member size for the purpose of securing a seismic intensity of 0.45G or more by conventional methods with construction methods in which earthquake-proof reinforcement is not applied, the ultimate strength is increased by applying steel material to pipe racks that are designed for a seismic intensity of 0.3G.

(5) Applying items (1) - (4) to new pipe rack construction will have the effect of reducing the

amount of steel used by one-third.

In regard to the content above, the EPR (**E**arthquake-**p**roof **R**einforcement) system was devised in order to realize the earthquake-proof reinforcement of existing pipe racks. If this system is used, it will facilitate the selection of the locations for reinforcement, the determination of the total amount of steel required for the reinforcement locations, the size of the pedestal reinforcement and so forth. In addition, it will also eliminate the need to conduct structural calculations after enforcing the earthquake-proof reinforcement. Consequently, a broad reduction in the labor used in the reinforcement operation will also be realized.

REFERENCES

1) 1995 [Disaster of Hanshin great earthquake string motion] Architecture Magazine Vol.37 No.457
2) 1951.[The behavior of framed structure under repeated loading] B.G. Neal quart. J. Mech. Appl. Math.
3) 1984 [Effect of sample preparation method on cyclic undrained strength of sand triaxial and torsion tests] Fumio Tatsuoka etc. Bulletin of ERS, No.17 Univ. of Tokyo
4) 1962 [Automatic analysis and design plastic frame] Hisashi Tanaka Bulletin of ERS, No.17 Univ. of Tokyo
5) 2000 [The regulation of earthquake-proof design on equipments of high pressure gas, level 2] Japan High Pressure Gas Association KHK E 012-3-2000, KHK E 012-4-2000